Crystal structures and growth mechanism for ultrathin films of ionic compound materials: FeO(111) on Pt(111)

W. Ranke, M. Ritter, and W. Weiss
Fritz-Haber-Institut der Max-Planck-Gesellschaft, Faradayweg 4-6, 14195 Berlin, Germany
(Received 28 December 1998)

The growth and atomic structures of epitaxial iron-oxide films on Pt(111) were studied with scanning tunneling microscopy and high-resolution low-energy electron diffraction. During the initial layer-by-layer growth of FeO(111) four different structures are formed as the coverage increases to 2.5 monolayers, then a three-dimensional growth of $Fe_3O_4(111)$ islands begins. The structural transformations demonstrate that the relaxations within the FeO(111) films and the Stranski-Krastanov growth mode are induced by electrostatic surface energies, which dominate the energetics of thin film systems made up of ionic compound materials. [S0163-1829(99)11827-7]

The growth of epitaxial thin films is of great importance for many basic research studies and technological applications. New materials with novel properties can be obtained in the form of ultrathin films with modified crystal structures. Great efforts are put into the preparation of thin metal-oxide films, which serve as model systems for fundamental surface science and catalysis studies.[1–3] For all applications the control of the film structure and morphology is crucial. Whereas a detailed picture of the atomic scale processes during heteroepitaxial growth has evolved for metals[4] and semiconductor materials,[5] not much is known about ionic compound materials like metal oxides in this respect.

If heteroepitaxial growth takes place close to equilibrium conditions, the growth mode depends on the surface free energies of the substrate γ_s and the film γ_f, as well as on the interfacial energy $\gamma_{i,n}$.[6] In the case of pseudomorphic growth $\gamma_{i,n}$ also contains the elastic energy of the strained film and therefore increases with the number of layers n. The surface energy of the strained film γ_f does not depend on the film thickness for metal and semiconductor materials studied so far. This often results in a Stranski-Krastanov growth where the initial pseudomorphic layer-by-layer growth is limited to a critical film thickness by the elastic energy. Then a three-dimensional growth of unstrained islands with dislocations at the substrate-overlayer interface or of coherently strained islands with limited sizes becomes favorable.[5]

In this work the growth of iron oxides onto Pt(111) is investigated on an atomic and mesoscopic scale. Previous investigations revealed four different atomic FeO(111) structures to occur during the initial growth,[7] and the lattice parameters of the last unknown structure could be clarified here. The entire data give new insight into the energetics of thin film systems of ionic compound materials, and they reveal a novel mechanism that determines the atomic structures and epitaxial growth mode of such systems. In contrast to metals and semiconductors, interfacial and elastic strain energies $\gamma_{i,n}$ play no significant role any more; instead electrostatic surface energies $\gamma_{f,n}$, which now depend on the number of layers n, dominate the energetics of the system.

The experiments were performed in two ultrahigh vacuum chambers with base pressures of 10^{-10} mbar in order to combine scanning tunneling microscopy (STM) with high-resolution low-energy electron diffraction (LEED) measurements, where the latter allowed us to determine lateral lattice constants with an accuracy of 0.01 Å.[3,7] Onto a clean Pt(111) surface prepared by numerous sputter-annealing cycles iron-oxide films were grown by repeated cycles of iron deposition at room temperature and subsequent oxidation at $T=870$ K in 10^{-6} mbar oxygen.[7] All STM measurements were performed at room temperature in the constant current mode.

Figure 1 shows large scale (left) and atomic resolution STM images (right) of consecutive iron-oxide growth stages. The large scale images reveal a layer-by-layer growth up to 2.1 monolayers (ML) of coverage. At submonolayer coverage (a) two monoatomic substrate steps indicated by the arrows are visible, and bare platinum substrate areas coexist with iron-oxide covered areas. In (b) the first iron-oxide layer is completed and hexagonally shaped second layer islands with diameters around 200 Å have formed. The second layer growth has proceeded in (c) and is completed in (d), where some third layer islands have formed. At this growth stage three-dimensional $Fe_3O_4(111)$ islands start to grow with the bulk lattice constant of this oxide.[7] All oxide overlayer steps in Fig. 1 run along the $[01\bar{1}]$ and $[\bar{1}10]$ directions of the substrate surface and exhibit height differences around 2.1 Å.

During this layer-by-layer growth four different atomic film structures are formed, which are displayed in atomic resolution STM images on the right side of Fig. 1. They are denoted 1–4 according to the sequence of their appearance, and their formation areas on the first three layer surfaces are indicated by the numbers in the large scale images on the left side. All structures exhibit protrusions forming hexagonal surface lattices with the unit cells indicated by the diamonds, which are about 3 Å in size. The STM image of structure 2 was observed previously by Galloway, Benitez, and Salmeron.[8] An image simulation based on quantum-chemistry electron-scattering theory revealed the short periodicity protrusions to occur at oxygen atom positions located in the topmost layer of this film, and the model shown in Fig. 2 was proposed.[9] It consists of a hexagonal close-packed iron-oxygen bilayer with oxygen located on top, which is laterally expanded to a lattice constant of $a_{FeO}=3.09$ Å (the

 ©1999 The American Physical Society

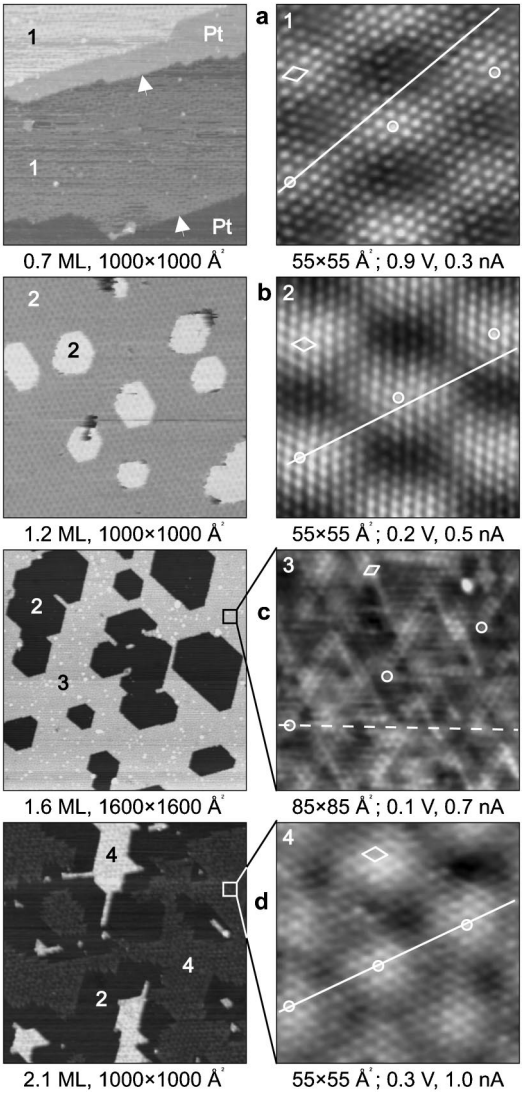

FIG. 1. Large scale (left) and atomic resolution (right) STM images of epitaxial FeO(111) films on Pt(111). Four different coincidence structures 1–4 are formed sequentially as the coverage increases. They exhibit different contrasts in the large scale images as indicated by the numbers.

value in bulk FeO is 3.04 Å) and rotated by $\alpha = 0.6°$ against the Pt(111) surface lattice. This creates the moiré superstructure cell observed in the atomic resolution STM image, which can be defined by the coincidence site 2 chosen arbitrarily on top of an underlying platinum atom. The lattice constant of $a_{FeO} = 3.09$ Å indeed is revealed by the FeO(10) spot position in the high-resolution LEED pattern,[7] and the model was further confirmed by photoelectron diffraction experiments.[10]

Analogous to structure 2, the protrusions in the atomic resolution images of the other structures also are attributed to topmost layer oxygen atom positions. Thus all FeO(111) films form purely oxygen-terminated surface structures as depicted in Fig. 2. In this rigid model structures 1, 2, and 4 with their corresponding coincidence sites are obtained for FeO(111) bilayers with the lateral lattice constants a_{FeO} and misfit angles α listed in Table I, which were determined experimentally by high-resolution LEED measurements and which almost exactly coincide with the values obtained theo-

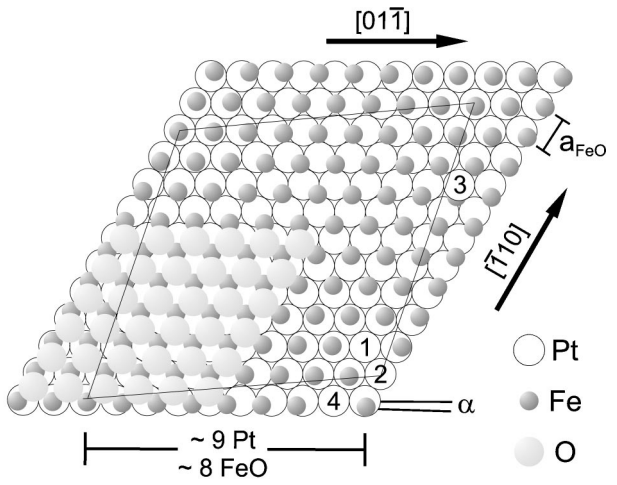

FIG. 2. Rigid model of the four FeO(111) structures formed on Pt(111). FeO(111) bilayers with different lattice constants a_{FeO} and rotated against the platinum surface lattice by different angles α lead to coincidence sites 1–4. Here coincidence structure 2 with its superstructure cell is shown.

retically from the rigid models in Fig. 2.[7] The corresponding moiré angles of these models also agree well with those observed by STM.

Structure 3 is not characterized by a simple moiré superstructure but by triangular features which appear with a periodicity of 38.4 Å along directions rotated by ±30° against the atom rows on Pt(111). This corresponds to a $(8\sqrt{3} \times 8\sqrt{3})\ R30°$ superstructure with respect to Pt(111) as indicated by coincidence site 3 in Fig. 2. However, structure 3 is observed in the second layer and is assumed to form on top of structure 4 located in the first layer underneath, because structure 4 forms a simple superstructure both with respect to Pt(111) and structure 3. Structure 3 exhibits considerable short-range disorder and not all oxygen atoms occur at equivalent positions within the different triangles. The best defined oxygen atom positions are aligned along the bright rows in the STM image and form the triangle edges. They are represented as black circles in Fig. 3. The triangles were arranged so that all corners occupy equivalent positions with respect to the (8×8) unit cell of structure 4 underneath (in-

TABLE I. Experimentally determined lateral lattice constants a_{FeO}, rotation misfit angles against the Pt(111) surface lattice α, and Fe-O(111) interlayer distances of the four FeO(111) structures formed in the first three layers. The Fe-O bond lengths were calculated from a_{FeO} and the interlayer distances.

Structure, layer	a_{FeO} (Å)	Misfit angle α	Fe-O interlayer distance	Fe-O bond length (Å)
S1, 1st layer	3.11	1.3°		
S2, 1st layer	3.09	0.6°	0.68	1.91
S2, 2nd layer	3.09	0.6°	1.05	2.1
S3, 2nd layer	3.40[a]		<1.05	
S4, 3rd layer	3.15	0°	1.05	2.1
FeO bulk	3.04		1.25	2.16

[a]Average value.

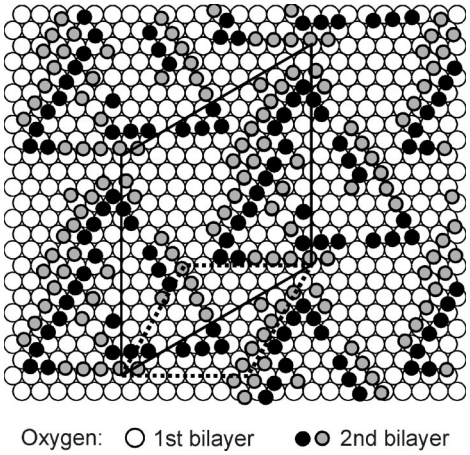

FIG. 3. Model of the ''triangle'' structure 3 formed in the second layer on top of structure 4 in the first layer. The $(8\sqrt{3}\times 8\sqrt{3})$ and (8×8) superstructure cells of structures 3 and 4 are indicated by the solid and dotted lines, respectively.

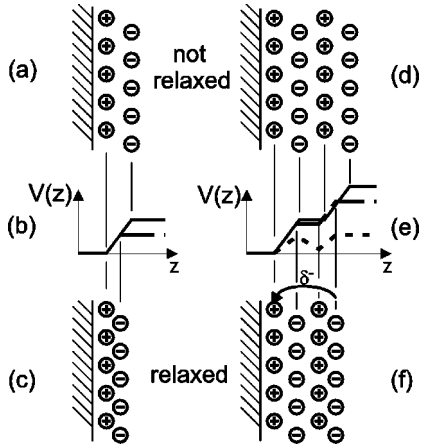

FIG. 4. Schematic side view representation of one and two bilayer thick films of an ionic material on top of a metal substrate. The electrostatic potential $V(z)$ for unrelaxed and relaxed overlayers are indicated by the solid and broken lines, respectively (z is the distance from the substrate surface). The dotted line indicates the potential after a charge redistribution of δ^- has occurred within the overlayer.

dicated by the dotted lines), and the large black oxygen atoms occupy hollow site positions with respect to the first FeO bilayer which correctly continue the NaCl type lattice. The grey oxygen atoms are on ''wrong,'' mostly near-bridge positions. This causes a more open packing with interatomic distances between that of structure 4 (3.17 Å) and values as large as 3.8 Å. The LEED spot positions of structure 3 correspond to a lattice constant of 3.4 Å, which can be considered as an average interatomic distance. Within the areas in Fig. 3 where no second layer atoms are plotted the atom positions could not be determined due to the lack of clear intensity maxima in the STM images.

All FeO(111) lattice constants a_{FeO} listed in Table I are larger than the FeO bulk value, and for coverages above 1.5 ML they increase in the second layer when compared to the first layer. This is an unexpected behavior because the Pt(111) surface lattice constant (2.77 Å) is considerably smaller than the FeO bulk value (3.04 Å). Instead of adopting the FeO bulk structure with increasing film thickness the lateral expansion increases, and the increasing elastic strain energy must be overcompensated by another stabilizing contribution. The lateral expansions are accompanied by reduced interlayer distances as listed in Table I. For structure 2 formed in the first layer an interlayer distance of 0.68 Å was deduced from photoelectron diffraction measurements.[10] An interlayer distance of 1.05 Å is deduced for structures 2 and 4 in the second and third layer, respectively, as deduced from the height differences between consecutive layers with equal surface structures measured by STM. The interlayer distance of the strongly expanded structure 3 is assumed to be even smaller.

Structures 1, 2, and 4 do occur in the first FeO(111) layers and represent slightly different substrate-overlayer interface geometries. This indicates that the interfacial energy does not depend critically on the exact geometry formed at the interface to the substrate. Although an exact description of the film energetics would require *ab initio* total energy calculations, the observed relaxations can be understood qualitatively when considering the ionic character of the oxide material. All FeO(111) films form polar unreconstructed surfaces terminated by close-packed oxygen layers. In a purely ionic model as formulated by Tasker[11] each iron-oxygen bilayer produces an electric field which increases the surface potential of the oxide film $V(z)$ (z is the distance from the substrate surface). This results in a surface energy $\gamma_{f,n}$ that increases with the number of layers n as illustrated schematically in Fig. 4 for one (a)–(c) and two (d)–(f) bilayer thick films. Since the potential variation $V(z)$ within each bilayer is proportional to the interlayer distance indicated by the solid lines, the surface energy of the films can be decreased by relaxations that reduce the interlayer distances. This situation is depicted in Figs. 4(c) and 4(f) and by the broken lines in Figs. 4(b) and 4(e).

The electrostatic surface energy is the driving force for the reduction of the Fe-O interlayer distances in the FeO(111) films and the structural transformations observed. Since reduced interlayer spacings would reduce the Fe-O bond lengths, the films respond by increasing their lateral lattice constants. The resulting Fe-O bond lengths in the second and third FeO layers are 2.1 Å, slightly smaller than the FeO bulk value of 2.16 Å (see Table I). The interlayer distance for structure 2 in the first layer (0.68 Å) results in an Fe-O bond length of 1.91 Å, which corresponds to a value expected for adsorbed oxygen as observed on rhodium.[12] This indicates a reduced ionic charge in the first bilayer, which must be induced by a charge redistribution within the overlayer as indicated by the δ^- in Fig. 4(f). Such a charge redistribution further decreases the surface energy[13] as indicated by the dotted line in Fig. 4(e).

That a thickness-dependent electrostatic surface energy $\gamma_{f,n}$ dominates the total energy of the system also is reflected by the sequence of structural transformations visible in the large scale STM images in Fig. 1. At submonolayer coverages structure 1 is formed. Because a second bilayer considerably increases the surface energy, the system tries to avoid its formation and forms the slightly compressed structure 2 just before the first layer gets completed. Then the second layer starts to grow with structure 2, and the surface energy of the film strongly increases with the second layer coverage.

This is the driving force for the transformation of structure 2 into structure 3, which takes place at coverages around 1.5 ML. In this extremely expanded structure with O-O distances up to 3.8 Å topmost oxygen atoms relax deeply into the underlying iron layer, leading to a strongly reduced Fe-O interlayer distance. Before the second layer gets completed structure 3 transforms into the more compressed structure 4, because again the system tries to avoid the formation of the next layer. Then third layer islands with structure 4 start to grow. As can be seen in the large scale STM image in Fig. 1(d) the more compressed structure 2 forms around these third layer islands. Again the system tries to incorporate as much material as possible into the first two bilayers in order to avoid the third layer growth. The maximal FeO coverage is 2.5 ML, then the growth of $Fe_3O_4(111)$ islands forming a more stable surface structure becomes favorable.[14]

In summary, iron oxide grows in a Stranski-Krastanov mode onto Pt(111) with two closely related crystal structures involved, FeO and Fe_3O_4. The initial FeO layer-by-layer growth is limited to a maximal thickness of 2.5 ML, then a three-dimensional growth of $Fe_3O_4(111)$ islands becomes favorable. This growth mode and the large relaxations within the ultrathin FeO(111) films are caused by the electrostatic FeO(111) surface energy which increases with the number of layers *n*, whereas interfacial and elastic strain energies play no significant role. This represents a new mechanism that dominates the energetics of thin film systems of ionic materials and that determines their growth mode and crystal structures. Ultrathin films with polar surface orientations always reduce their interlayer distance, resulting in laterally expanded structures, which recently also was observed for α-$Fe_2O_3(0001)$ grown onto $Al_2O_3(0001)$ substrates.[15]

We thank M. Swoboda for technical assistance and the Deutsche Forschungsgemeinschaft for financial support.

[1] H.-J. Freund, Angew. Chem. **109/5**, 444 (1997).
[2] S. C. Street, C. Xu, and D. W. Goodman, Annu. Rev. Phys. Chem. **48**, 43 (1997).
[3] W. Weiss, M. Ritter, D. Zscherpel, M. Swoboda, and R. Schlögl, J. Vac. Sci. Technol. A **16**, 21 (1998).
[4] H. Brune, Surf. Sci. Rep. **31**, 121 (1998).
[5] E. Pehlke, N. Moll, A. Kley, and M. Scheffler, Appl. Phys. A: Mater. Sci. Process. **65**, 525 (1997).
[6] E. Bauer and J. H. van der Merve, Phys. Rev. B **33**, 3657 (1986).
[7] M. Ritter, W. Ranke, and W. Weiss, Phys. Rev. B **57**, 7240 (1998).
[8] H. C. Galloway, J. J. Benitez, and M. Salmeron, Surf. Sci. **298**, 127 (1993).
[9] H. C. Galloway, P. Sautet, and M. Salmeron, Phys. Rev. B **54**, R11 145 (1996).
[10] Y. J. Kim, C. Westphal, R. X. Ynzunza, H. C. Galloway, M. Salmeron, M. A. Van Hove, and C. S. Fadley, Phys. Rev. B **55**, R13 448 (1997).
[11] P. W. Tasker, J. Phys. C **12**, 4977 (1979).
[12] S. Schwegmann, H. Over, V. De Renzi, and G. Ertl, Surf. Sci. **375**, 91 (1995).
[13] C. Noguera, *Physics and Chemistry at Oxide Surfaces* (Cambridge University Press, Cambridge, England, 1996).
[14] W. Weiss and M. Ritter, Phys. Rev. B **59**, 5201 (1999); M. Ritter and W. Weiss, Surf. Sci. (to be published).
[15] S. Chambers (private communication).